ASEG-PESA 2015
Geophysics and Geology together for Discovery
24th International Geophysical Conference and Exhibition
15–18 February 2015 Perth, Western Australia

3D joint inversion of gravity gradiometry and magnetic data in spherical coordinates with the cross-gradient constraint

Haoran Wang
China Uni. of Geosciences (Wuhan)
388 Lumo Road, Hongshan District
Wuhan 430074, P. R. China
whr.cug@gmail.com

Yaoguo Li
Colorado School of Mines
1500 Illinois Street, Golden
CO 80401, USA
ygli@mines.edu

Chao Chen
China Uni. of Geosciences (Wuhan)
388 Lumo Road, Hongshan District
Wuhan 430074, P. R. China
chenchao@cug.edu.cn

SUMMARY

Earth observing satellites offer exciting new opportunities to study the large-scale regional or global lithospheric structures by producing reliable potential-field data sets including gravity, gravity gradiometry, and magnetic data that are publicly accessible. Joint inversions may offer an effective means of utilizing these different types of data to improve the construction lithospheric models. In this paper, we develop a joint inversion algorithm for satellite gravity gradiometry and magnetic data in the spherical coordinates for simultaneously constructing the density and susceptibility distributions in the lithosphere. Given the undetermined relationship between the two different physical properties, we apply the cross gradient to constrain the two recovered models so they structurally similar. We use a synthetic data example to illustrate the algorithm and its potential benefits. We will also demonstrate the algorithm by applications to field data sets in the presentation.

Key words: joint inversion, cross-gradient, gravity gradiometry, magnetic anomaly, spherical coordinates.

INTRODUCTION

The GOCE satellite has delivered a large set of valuable global gravity gradient data with its highly sensitive gravity gradiometer. As the ESA's SWARM mission progresses, the upcoming Earth's magnetic field data set will provide us with more information about the Earth's interior complementary to the GOCE data. With the availability of such global-scale potential-field data, we can examine the large-scale regional lithospheric structure. Carrying out physical property inversions is one approach to achieve this objective.

There are two challenges to this approach. The first is the inversion of such data by taking into account the curvature of the earth. There have been many efforts in this area by formulating the modelling and inversion in the spherical coordinates. In particular, Liang et al. (2014) develop a method for 3D inversion of gravity data in spherical framework by extending the work of Li and Oldenburg (1996) in the Cartesian coordinates. Du et al. (2013) develop a spherical magnetic inversion algorithm using a similar formulation.

The second challenge is how to simultaneously utilize the information contained in these two complementary data, namely, gravity gradiometry and magnetic data sets. A joint inversion appears to be a logical choice. The difficulty lies in the lack of a definable relationship between density and magnetic susceptibility or magnetization. Since density and magnetic properties are associated with the specific geologic structures in the same region, structure similarity could be used to link the two separate physical properties. For this purpose, Gallardo and Meju (2003) have developed a cross-gradient inversion technique that enforces the similarity in the gradients of the recovered models. We apply that approach to the joint inversions of satellite data by extending the cross-gradient to the spherical coordinates.

In this paper, we construct the discretised cross-gradient function in the spherical coordinates to make a linkage between the large-scale distributions of density and susceptibility. As a constraint, the new cross-gradient function is appended to the total objective function in classic Tikhonov regularized inversion. In addition, we impose bound constraints on the recovered density contrast and magnetic susceptibility. The final nonlinear minimization is solved by Gauss-Newton method.

INVERSION IN SPHERICAL COORDINATES

In order to carry out joint inversion, we first describe the inversion of individual data set in the spherical coordinates in this section.

We first divide the subsurface region of interest into a set of tesseroid cells using a 3D mesh in latitude, longitude, and radius. For either gravity gradient data or the magnetic data without self-demagnetization, the forward modelling is a linear relationship between the observed data and the physical properties in tesseroid cells. The equation can be expressed by:

$$\mathbf{d} = \mathbf{G}\mathbf{m} \tag{1}$$

where $\mathbf{d}$ is the observation data vector, $\mathbf{G}$ is the kernel matrix, and $\mathbf{m}$ is the model parameter vector. We use $\mathbf{d}_1$, $\mathbf{m}_1$, and $\mathbf{G}_1$ to denote gravity gradiometry data, density model, and corresponding kernel matrix, respectively. Similarly, $\mathbf{d}_2$, $\mathbf{m}_2$, and $\mathbf{G}_2$ denote the magnetic data, susceptibility model, and kernel matrix. There is no closed-form solution for the field due to a tesseroid cell, so we adopt the Gauss-Legendre quadrature integration to calculate the entries of the kernel matrices of both gravity gradient and magnetic anomaly (e.g., Asgharzadeh et al., 2007).

Given a set of data $\mathbf{d}_l^{obs}$ ($l = 1,2$ denoting the gravity gradient and magnetic problem, respectively) and the above definition of forward modelling in equation 1, the individual inversion of either data set can be solved using a Tikhonov regularisation formalism and expressed as an optimization problem of the following,

$$\Phi_{rl}\left(\mathbf{m}_1\right) = \left\| \mathbf{W}_{dl}(\mathbf{d}_l^{obs} - \mathbf{G}_l \mathbf{m}_l) \right\|^2 + \beta_l \left\| \mathbf{W}_{ml}(\mathbf{m}_l - \mathbf{m}_l^{ref}) \right\|^2, \quad (2)$$

where $\mathbf{W}_{dl}$ is the data weighting matrix whose diagonal elements are the inverse of the data standard deviations, β_l the regularization parameter, and $\mathbf{m}_l$ and $\mathbf{m}_l^{ref}$ are respectively the unknown model to be recovered and the reference model. The model weighting matrix $\mathbf{W}_{ml}$ is the discretised representation of the model objective function in the spherical coordinates.

Liang et al. (2014) adopt a form of model objective function commonly used in the exploration community and it consists of a smallest model component and flatness components in three orthogonal spatial directions. A radial weighting similar to the depth weighting (e.g., Li and Oldenburg, 1996) is also used to deal with the natural decay of the kernel. The same approach is used by Du et al. (2013) in the inversion of magnetic data in spherical coordinates. We use the same type of objective function in this study.

The kernels of gravity gradiometry data and magnetic data decays in the same manner with the depth (in the radial direction), so their common weighting function in the inversion is given by

$$w^2(r) = \frac{1}{(H + R - r)^3} \cdot \frac{r}{R} \quad (3)$$

where R is the average radius of Earth's surface, r the radius of the centre of a tesseroid cell, H the height of observation.

In potential-field inversions, it is common to impose lower and upper bounds on the recovered model to ensure that the inverted model has values in the range that is either realistic in general or prescribed from known geological information. For this reason, we also build in a component in the inversion algorithm for the constraint $\mathbf{l} \le \mathbf{m} \le \mathbf{u}$, where $\mathbf{l}$ and $\mathbf{u}$ represent the lower and upper bounds for model parameters. These bounds are different for density and susceptibility, but also can vary from cell to cell. We implement these constraints using the primal logarithmic barrier method (Nocedal and Wright, 2006) by including the following barrier term in the objective function in equation 2,

$$\Phi_b(\mathbf{m}) = -2\lambda \sum_{j=1}^{M} \left[\ln \frac{m_j - l_j}{u_j - l_j} + \ln \frac{u_j - m_j}{u_j - l_j} \right]$$

(4)

where λ is the log barrier parameter, $\mathbf{m}$ can be either density contrast or susceptibility, and M is the number of model parameters.

The above algorithm is well understood and can be used to invert either gravity gradient or magnetic data separately. They also form the essential building block of joint inversion of the two data sets. The key is to form a linkage between the density contrast model and susceptibility model. We proceed to this aspect in the next section.

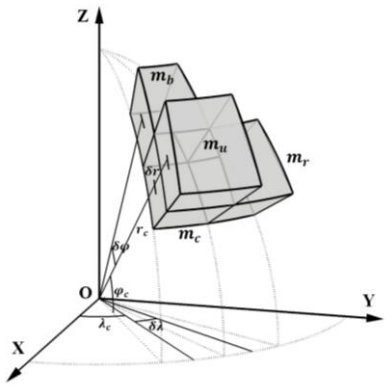

Figure 1. Tesseroid cells related to finite differences with three directions in spherical coordinates

CROSS-GRADIENT IN SPHERICAL COORDINATES

Let us now consider the joint inversion of the two data sets. As mentioned in the Introduction, we choose to impose the structure similarity between density and susceptibility models through the 3D cross-gradient function. This approach is first developed by Gallardo and Meju (2003). The cross product of the gradient vectors of the two models measure the dissimilarity between the boundaries or spatial variations in the two models, so minimizing the absolute values of the cross product will likely encourage the two models to attain similar structure. The cross-gradient function is given by

$$\vec{t}(x, y, z) = \nabla m_1(x, y, z) \times \nabla m_2(x, y, z) \quad (5)$$

Although the original method was developed for Cartesian coordinates, it can be easily extended to the spherical coordinates by using the corresponding spatial gradient operator

$$\nabla(r, \varphi, \lambda) = \frac{\partial}{\partial r}\mathbf{e}_r + \frac{1}{r}\frac{\partial}{\partial \varphi}\mathbf{e}_\varphi + \frac{1}{r\cos\varphi}\frac{\partial}{\partial \lambda}\mathbf{e}_\lambda \quad (6)$$

where r, φ, λ are respectively the radius, latitude, and longitude in the geocentric spherical coordinates, $\mathbf{e}$ represent the unit vectors in the three direction.

Following the definition of cross gradient in the Cartesian coordinates presented by Fregoso and Gallardo (2009) using four adjacent model cells, we define the spherical version using four tesseroid cells shown in Figure 1,

$$\begin{aligned}
t_\varphi &= \frac{4}{r_c \cos\varphi_c \delta\lambda\delta r}\left[m_{1u}(m_{2c} - m_{2b}) + m_{1c}(m_{2b} - m_{2u}) \right. \\
&\quad \left. + m_{1b}(m_{2u} - m_{2c})\right] \\
t_\lambda &= \frac{4}{r_c \delta\varphi\delta r}\left[m_{1u}(m_{2r} - m_{2c}) + m_{1c}(m_{2u} - m_{2r}) \right. \\
&\quad \left. + m_{1r}(m_{2c} - m_{2u})\right] \\
t_r &= \frac{4}{r_c^2 \cos\varphi_c \delta\lambda\delta\varphi}\left[m_{1c}(m_{2r} - m_{2b}) + m_{1r}(m_{2b} - m_{2c}) \right. \\
&\quad \left. + m_{1b}(m_{2c} - m_{2r})\right]
\end{aligned} \quad (7)$$

This yields a cross gradient vector at each model cell, and we can then define the cross-gradient objective function by the L2 norm,

$$\Phi_t(\mathbf{m}_1, \mathbf{m}_2) = \frac{\mu}{2}\left\|\mathbf{t}(\mathbf{m}_1, \mathbf{m}_2)\right\| \tag{8}$$

where μ is the cross-gradient parameter for including the cross-gradient objective function into the total objective functions to be minimized. The value of μ determines the strength of the constraint.

We are now ready to state the joint inversion of the gravity gradient data and magnetic data using a cross-gradient constraint. The total objective function to be minimized for the solution is the sum of the Tikhonov objective functions in equation 2, the two barrier functions in equation 4, and the cross-gradient objective function in equation 8,

$$\Phi(\mathbf{m}) = \sum_{l=1}^{2}\left[\Phi_{rl}(\mathbf{m}_l) + \Phi_b(\mathbf{m}_l)\right] + \Phi_t(\mathbf{m}_1, \mathbf{m}_2) \tag{9}$$

We note that the only linkage between the two inversions is the cross-gradient term $\Phi_t(\mathbf{m}_1, \mathbf{m}_2)$.

Minimizing the objective function in equation 9 yields the desired models with structural similarity. The degree of similarity between the models is determined by both the information content in the two data sets and the cross-gradient parameter. Removing the cross-gradient term (i.e., $\mu = 0$) leads to two separate inversions.

Equation 9 is non-quadratic in two model vectors. Therefore, the minimization must be carried out iteratively. We apply Gauss-Newton method to achieve this. At the k'th iteration, we solve a linear system of equations to obtain the model perturbation. To simply the presentation, we introduce the following notation,

$$\mathbf{m} = \begin{bmatrix}\mathbf{m}_1\\ \mathbf{m}_2\end{bmatrix}, \mathbf{d}^{obs} = \begin{bmatrix}\mathbf{d}_1^{obs}\\ \mathbf{d}_2^{obs}\end{bmatrix}, \tag{10}$$

$$\mathbf{G} = \begin{bmatrix}\mathbf{W}_{d1}\mathbf{G}_1 & \\ & \mathbf{W}_{d2}\mathbf{G}_2\end{bmatrix}, \quad \mathbf{W}_{\mathbf{m}} = \begin{bmatrix}\beta_1\mathbf{W}_{m1} & \\ & \beta_2\mathbf{W}_{m2}\end{bmatrix} \tag{11}$$

With this notation, the system of equations to be solved for the model perturbation $\Delta\mathbf{m}$ is given by

$$\begin{aligned}&\left[\mathbf{G}^T\mathbf{G} + \mathbf{W}_m^T\mathbf{W}_m + \mu(\mathbf{B}^{(k)})^T\mathbf{B}^{(k)} + \lambda\mathbf{X}^{-2} + \lambda\mathbf{Y}^{-2}\right]\Delta\mathbf{m}\\ &= \mathbf{G}^T(\mathbf{d}^{obs} - \mathbf{G}\mathbf{m}^{(k)}) - \mathbf{W}_m^T\mathbf{W}_m(\mathbf{m}^{(k)} - \mathbf{m}^{ref})\\ &\quad - \mu(\mathbf{B}^{(k)})^T\mathbf{t}^{(k)} + \lambda\mathbf{X}^{-1}\mathbf{e} - \lambda\mathbf{Y}^{-1}\mathbf{e}\end{aligned} \tag{12}$$

where $\mathbf{B}^{(k)}$ is the Jacobian of the cross-gradient function at the k'th iteration, $\mathbf{X}$ = diag $\{m_1\text{-}l_1, \ldots, m_{2M}\text{-}l_{2M}\}$, $\mathbf{Y}$= diag $\{u_1\text{-}m_1, \ldots, u_{2M}\text{-}m_{2M}\}$, $\mathbf{e} = \{1, \ldots, 1\}$.

In the basic form, we fix the two regularization parameters and the cross-gradient parameter μ. We start the iteration with a large log barrier parameter λ. In each log barrier step, solve equation (12) to obtain the model perturbation to update the model with the condition that the model remains within the bounds. We then reduce the λ and proceed to the next iteration. The final solution is obtained by searching for the optimal regularization parameters. The choice of the cross-gradient parameter is slightly more flexible and a range of values can yield acceptable results.

SYNTHETIC EXAMPLE

To illustrate our algorithm, we use a synthetic density and a susceptibility model with similar geometries. The density contrast model consists of two anomalous blocks with differing values and different depth extents. The magnetic model consists of two blocks with the same dimensions and effective susceptibility. One of the magnetic bodies coincides with an anomalous density body, whereas the second magnetic body coincides with the top portion of the second density body. Thus, some boundaries in the two model occur at the same location but others boundaries are offset (Figure 2).

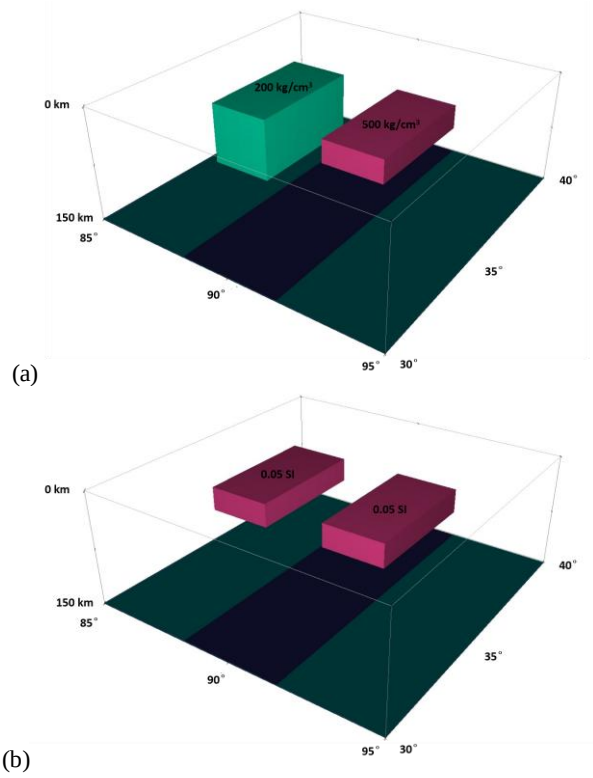

Figure 2. (a) Density model. (b)Susceptibility model.

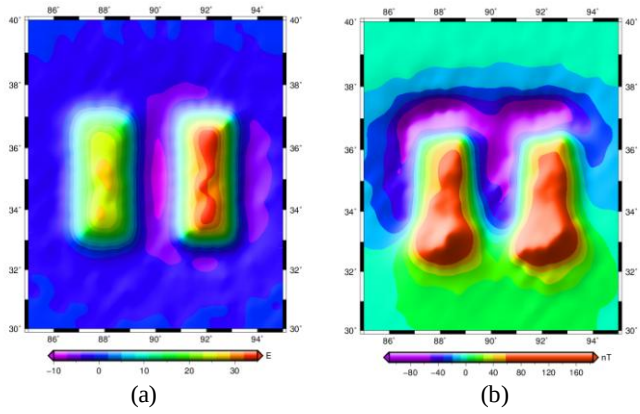

Figure 3. (a) Synthetic gravity gradient data Trr. (b) Total-field magnetic anomaly data.

For simplicity, we simulate only T_{rr} component of gravity gradient tensor and the total-field magnetic anomaly data (Figure 3). To illustrate the value of joint inversion, we generate the magnetic data by simulating the presence of unknown remanent magnetization but carry out the inversions assuming induced magnetization only. The remanent magnetization is simulated by using an effective susceptibility of 0.05 SI and magnetization direction whose inclination and declination are both shifted from those of the inducing field by -20°. The inducing field directions are calculated for assumed western China region from the IGRF11 model. This is a significant deviation and is expected to cause difficulties in the magnetic inversion. In addition, we add 10% Gaussian noise to simulate noisy data. In contrast, we contaminate the gravity gradient data with 3% noise. The two data sets are shown in Figure 3.

We first invert each data set separately. We impose a lower and upper bounds of 0 to 500 kg/m³ on the density, and 0 to 0.05 SI on the magnetic susceptibility. Vertical cross-sections through the inverted models are shown in Figure 4. We observe that the density bodies are recovered reasonably well, but the susceptibility bodies are too shallow and appear to spread out horizontally. The poor recovery is due to the influence of unknown remanent magnetization.

Next, we jointly invert the two data sets by imposing the cross-gradient constraint as described in the preceding section. The results are shown in the vertical sections in Figure 5. The recovered density contrast model is slightly better, but the susceptibility model shows marked improvement. The depth to the top is more consistent with the true model, there is much less lateral spreading, and the two anomalies show a clear separation.

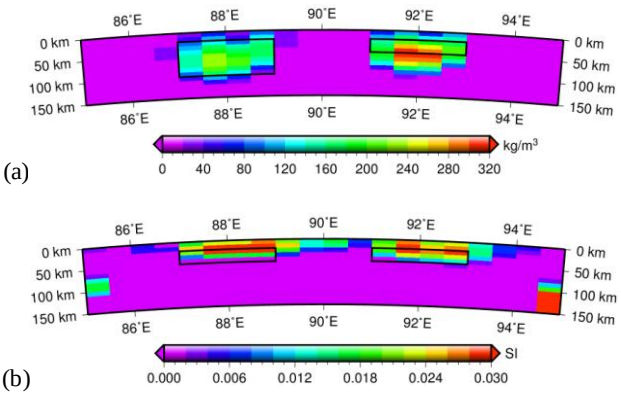

Figure 4. Vertical cross-section of recovered models from separate inversions. (a) Density model. (b)Susceptibility model. The black boxes outline the true position of the anomalous bodies.

CONCLUSIONS

We have developed an algorithm for joint inversion of gravity gradiometry and magnetic data using cross-gradient in the spherical coordinate system. The key component of the algorithm is the consistent use of the spherical coordinate gradient operator in the definition of the model objective function and of the cross-gradient operator. Synthetic model tests indicate that cross-gradient constraint is effective in the inversion of data sets with differing error characteristics and can help mitigate the adverse effect of unknown data errors such as those caused by erroneous assumptions about the presence of remanent magnetization. This approach may provide a path towards improved inversion of gravity gradient and magnetic data for regional studies using newly acquired satellite data.

ACKNOWLEDGMENTS

This research is supported by the Fundamental Research Funds for Institute for Geophysical and Geochemical Exploration, Chinese Academy of Geological Sciences (Grant Nos. WHS201211).

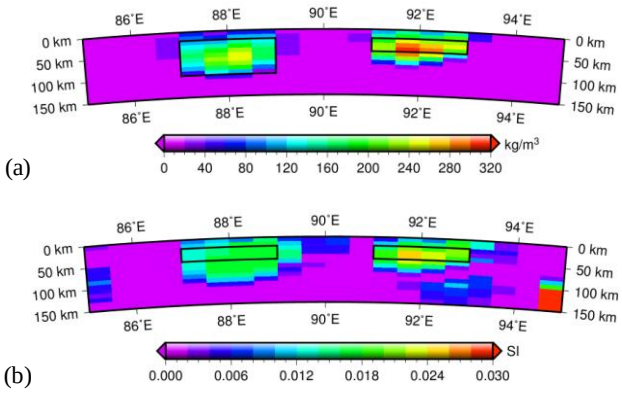

Figure 5. Vertical cross-section of recovered models using cross-gradient constraint. (a) Density model. (b)Susceptibility model.

REFERENCES

Asgharzadeh, M. F., von Frese, R. R. B., Kim, H. R., Leftwich, T. E., and Kim, J. W., 2007, Spherical prism gravity effects by Gauss-Legendre quadrature integration: Geophysical Journal International, 169, 1-11.

Du, J., Chen, C., Liang, Q., Wang, H., Li, Y., and Lane, R., 2013, 3-D inversion of the regional magnetic data in spherical coordinates and its preliminary application in Australia: ASEG Extended Abstracts 2013, 1, 1-4.

Fregoso, E., and Gallardo, L. A., 2009, Cross-gradients joint 3D inversion with applications to gravity and magnetic data: Geophysics, 74(4), L31-L42.

Gallardo, L. A., and Meju, M. A., 2003, Characterization of heterogeneous near-surface materials by joint 2D inversion of DC resistivity and seismic data: Geophysical Research Letters, 30(13), 1658.

Li, Y., and Oldenburg, D. W., 1996, 3-D Inversion of magnetic data: Geophysics, 61, 394-408.

Liang, Q., Chen, C., and Li, Y., 2014, 3-D inversion of gravity data in spherical coordinates with application to the GRAIL data: Journal of Geophysical Research, 119: 1359-1373.

Nocedal, J., and Wright, S., 2006, Numerical optimization, 2nd Edition, Springer, New York